ANALYSIS AND CHARACTERIZATION OF SOFT-LITHOGRAPHY-COMPATIBLE PARALLEL-ELECTRODE-SENSORS IN MICROFLUIDIC DEVICES

Ruxiu Liu, Chia-Heng Chu, Mert Boya, Dohwan Lee,
Ozgun Civelekoglu, Hang Chen and A. Fatih Sarioglu
Georgia Institute of Technology, Atlanta, USA

ABSTRACT

Microfluidic devices integrated with Coulter sensors have been widely used in counting and characterizing suspended particles. The electrodes in these devices are mostly arranged in a coplanar fashion due to a simple fabrication process and leads to non-uniform electric fields confined to the floor of the microfluidic channel. We have recently introduced a simple fabrication method that can effortlessly create parallel electrodes in microfluidic devices built with soft-lithography. In this paper, we theoretically and experimentally analyze the developed parallel-electrode Coulter sensor and compare its sensitivity with that of the Coulter sensor built on conventional coplanar electrodes. Both our simulation results and experiments with cell suspensions show that parallel-electrode Coulter sensor can provide as much as ~5× sensitivity improvement over conventional coplanar electrodes.

KEYWORDS

Microfluidics, soft lithography, Coulter sensor, resistive pulse sensing, coplanar electrode, parallel electrode

INTRODUCTION

Microfluidic devices with integrated electrical sensors excel at counting, sizing and characterizing micro/nanoparticles suspended in fluids [1,2]. The detection mechanism in these devices, known as the Coulter sensing or the resistive pulse sensing, relies on the modulation of impedance when a particle suspended in an electrolyte passes between two oppositely charged electrodes [3,4]. In most microfluidic devices, Coulter sensors are created by micromachined coplanar electrodes on the floor of microfluidic channels rather than utilizing the full channel geometry. While coplanar electrodes can be realized with a simple fabrication process that is compatible with the soft lithography, they not only generate non-uniform electric field affecting sensor performance, but also complicate the design of large-scale multiplexed electrical sensor networks (e.g., Microfluidic CODES sensors) [5-7], due to the need to route multiple electrode traces on a plane [8,9].

Use of counter-facing parallel electrodes in microfluidic channels can address the aforementioned problems. However, conventional approaches to build a parallel-electrode Coulter sensor in microfluidic devices typically rely on forming a glass-polyimide-glass sandwich structure [10], which not only involves complex fabrication process that requires a critical alignment between layers but also lacks the benefits of molded biocompatible polymers employed in the soft-lithography process. To address these issues, we recently introduced a soft-lithography-compatible fabrication method to create parallel-electrode Coulter sensors in microfluidic devices [11]. In our method, one of the electrodes of the Coulter sensor is formed by a thin metal film blanket-deposited on the inner walls of a microfluidic channel, while the other electrodes are lithographically patterned on the substrate according to the desired arrangement.

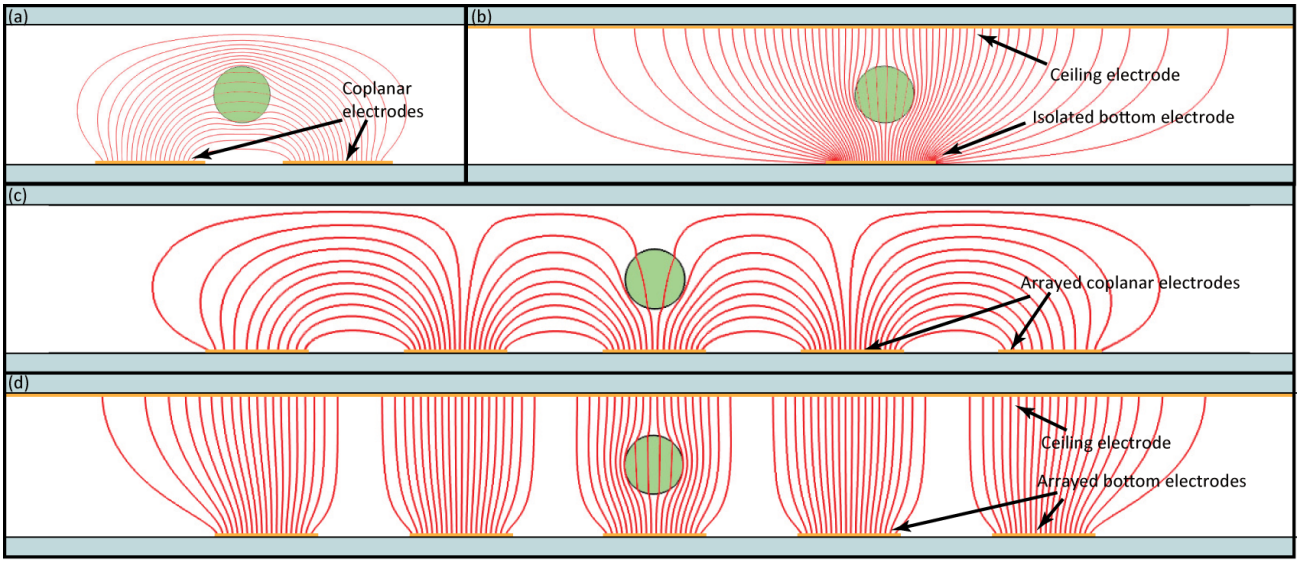

Figure 1: Simulation of the electrical field distribution generated by (a)(b) isolated coplanar (a) and parallel (b) electrode sensor, and (c)(d) arrayed coplanar (c) and parallel (d) electrode sensors fabricated using our approach.

In this paper, we comparatively analyze the performance of coplanar-electrode and parallel-electrode Coulter sensors using computer simulations and experiments. Specifically, we employ finite element analysis to simulate the electric field distribution within the microfluidic channel generated by those two sensors and calculate impedance variations for different particles. We also experimentally compare the performance of parallel-electrode and coplanar-electrode Coulter sensors by fabricating both sensors on the same microfluidic platform and use cell suspensions to verify simulation results.

FINITE ELEMENT ANALYSIS

We used COMSOL Multiphysics v5.3 AC/DC module to simulate Coulter sensor operation with coplanar or parallel electrode configurations and compared their performance. We first simulated electric field distribution within a microfluidic channel for different electrode configurations (Figure 1). When electric field distributions due to a single pair of coplanar electrodes (Figure 1a) and an electrode paired with a parallel blanket electrode (Figure 1b) are compared; while the parallel electrode configuration provides a more uniform electric field throughout the height of the microfluidic channel, it also leads to a broadened non-uniform field distribution due to fringing effects due to the size mismatch between ceiling and bottom electrodes. This fringing effect could partially be alleviated by arraying bottom electrodes, which limits the broadening of the field for the inner electrodes (Figure 1d) and provides a more uniform electrical distribution compared to arrayed coplanar electrodes (Figure 1c).

To quantitatively analyze the sensor performance, we calculated the electrical current flow in the microfluidic channel and compared the amplitude of electrical current modulation in response to particles flowing between the electrodes. For these calculations, we assumed phosphate buffer saline (PBS) as the electrolyte and human cells as suspended particles. Corresponding electrical parameters used in our simulations for modeling particle-electrode interaction are summarized in Table 1.

Table 1: Parameters used in computer simulations

Parameter	Value
Media conductivity	1.4 S m^{-1}
Media relative permittivity	80
Cytoplasm conductivity	0.5 S m^{-1}
Cytoplasm relative permittivity	60

We first calculated the decrease in electrical current as a measure of the sensor sensitivity for a 10 µm-diameter cell at multiple vertical positions in a 30 µm-wide microfluidic channel that is 15 µm- (Figure 2a), 35 µm- (Figure 2b), or 65 µm-high (Figure 2c). We considered three different electrode configurations: A coplanar electrode pair (Figure 1a), a surface electrode in parallel to a larger ceiling electrode (Figure 1b), and a surface electrode paired with an electrode that covers both the ceiling and the sidewalls of the microfluidic channel. Because the ceiling electrode extends over the sidewalls of the microfluidic channel with our fabrication technique, sidewalls need to be considered especially for a narrow microfluidic channel. In our 3D simulations, we assumed that the cells were flowing in the central streamline (i.e., center positioned 15 µm from each sidewall). We found the current modulation for the parallel-electrode sensor to be higher than the coplanar-electrode sensor for the same particle. The enhancement in sensitivity was more pronounced for cells at elevated vertical positions due to the electrical field being confined to the floor of the microfluidic channel for coplanar electrodes. We also observed that the extension of the ceiling electrode over the sidewalls increased the parallel-electrode sensitivity only when a cell was positioned below a crossover elevation.

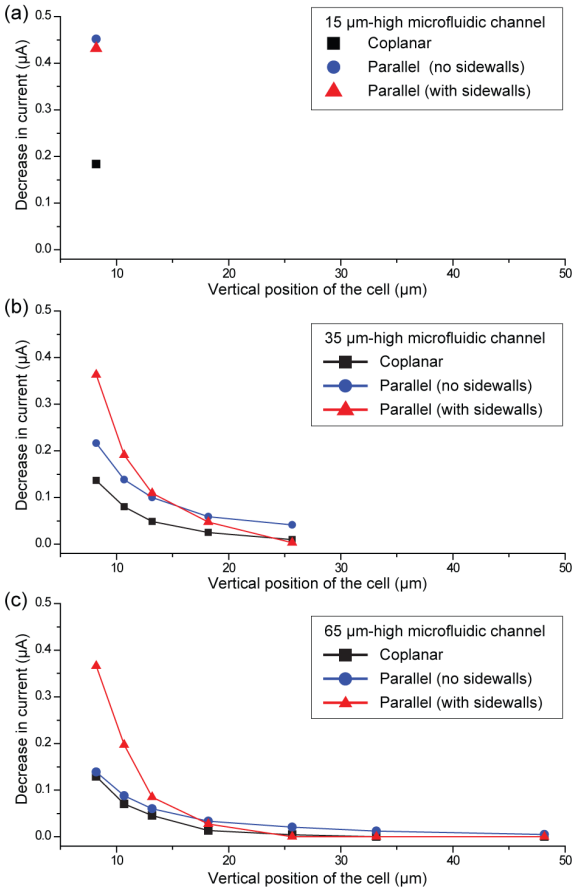

Figure 2: Simulated electrical current modulation in response to cells in microfluidic channels integrated with different electrode configurations. A 10 µm-diameter cell is positioned in the center streamline of the 30 µm-wide microfluidic channel with (a) 15 µm-, (b) 35 µm-, and (c) 65 µm-height. The current modulation is simulated for a cell at various vertical positions for each scenario.

We also investigated the effect of the cell size on the sensitivity of coplanar- and parallel-electrode sensors. We specifically compared the decrease in electrical current for the parallel- and coplanar-electrode configurations in a 35 µm-high and 30 µm-wide microfluidic channel for 6 µm-, 10 µm-, and 14 µm-diameter cells. Based on these simulations (Figure 3), we concluded that the sensitivity enhancement is higher for smaller cells (2~5× for 6 µm diameter cell) than larger cells (1.5~2× for 14 µm-diameter cell). In addition, the effect of the cell size on the sensitivity enhancement was found to be generally higher for cells at higher elevations in the microfluidic channel (Figure 3).

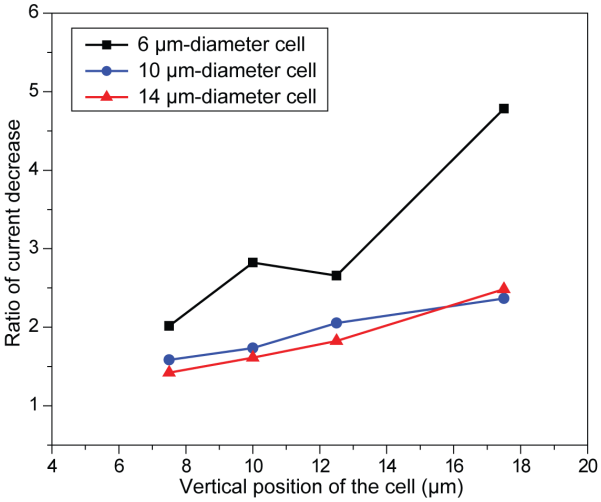

Figure 3: The ratio of the simulated current modulation between a parallel-electrode and a coplanar-electrode sensor. The ratio was calculated for different cell sizes at different elevations in a 30 μm-wide and 35 μm-high microfluidic channel.

DEVICE DESIGN AND FABRICATION

To experimentally compare the performance of coplanar- and parallel-electrode Coulter sensors, we created a microfluidic device that integrates two sensors based on coplanar electrodes and parallel electrodes along the same microfluidic channel (Figure 4). On the left side of the microfluidic channel, two 5 μm-wide coplanar electrodes separated by a 5 μm gap were created on the glass substrate. On the right side of the microfluidic channel, the inner walls of the microfluidic channel is coated with a gold film and only a single 5 μm-wide surface electrode was created on the glass substrate (Figure 4b). Because the same particle flowing in the microfluidic channel sequentially interacts both sensors, this experimental platform allowed us to directly compare signals from the two sensors.

The device consists of a glass substrate with micropatterned gold electrodes fabricated using a lift-off process and a polydimethylsiloxane (PDMS) microfluidic channel fabricated with a soft lithography process (Figure 5). A thin layer of negative photoresist was spun and patterned on a glass wafer using an optical lithography process, followed by the evaporation of a 20/80 nm Cr/Au stack. The wafer was then transferred to an acetone bath to remove the non-patterned region and diced into individual chips. The PDMS layer was created from a 15 μm-thick SU-8 mold patterned with photolithography. After the fluidic inlet, outlet and the electrical auxiliary holes were created using a biopsy punch, the inner walls of the PDMS microchannel was coated with a 500 nm-thick gold film with sputtering as coplanar-electrode-sensor-side (left side in Figure 4b) of the microfluidic channel was masked with a Kapton tape. Next, the coated PDMS substrate was transferred onto a sticky tape to selectively remove the gold sputtered on the surface to prevent short circuits while leaving the gold within the microfluidic channel intact. Next, the PDMS and glass substrates were activated in oxygen plasma, aligned under a microscope and bonded. Finally, we injected a conductive epoxy-coated wire from the auxiliary electrical port to form an electrical connection to the blanket electrode and created the final device.

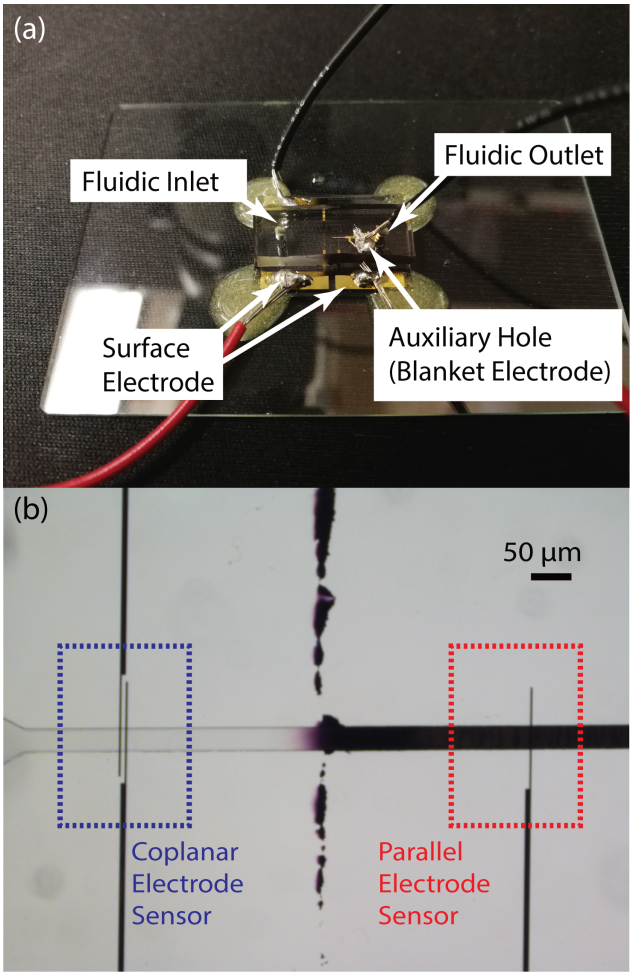

Figure 4: Images of the fabricated microfluidic device that contains both the coplanar- and parallel-electrode sensors. (a) A photo of the final device with fluidic and electrical connections and (b) a close-up microscope image of the two sensors formed along the same microfluidic channel.

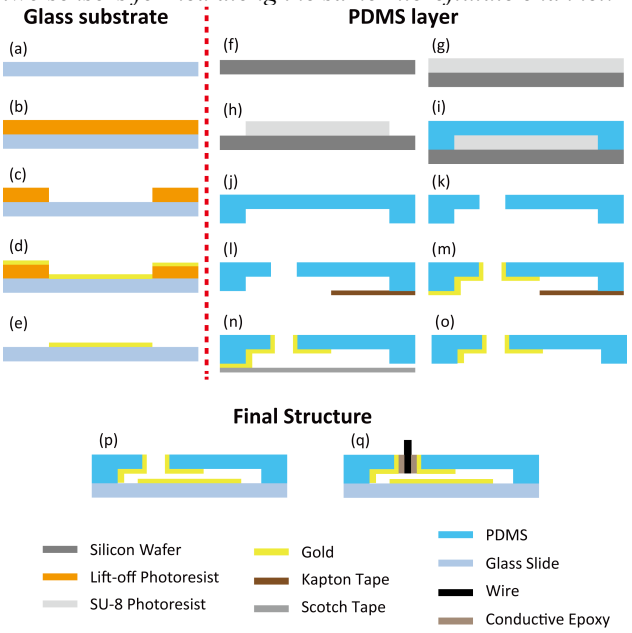

Figure 5: The fabrication process flow to create parallel

electrodes in a microfluidic device. (a)~(e) The fabrication of the glass substrate with micropatterned surface electrodes. (f)-(o) The fabrication of the metal-coated PDMS microchannel. (p)~(q) Bonding of the two components to form the final device.

EXPERIMENTAL RESULTS

We used cultured human breast cancer cells (MDA-MB-231) suspended in PBS as a sample to test our devices. The sample was driven through the microfluidic device using a syringe pump at a flow rate of 100 µL/h.

To measure the change in electrical impedance of the microfluidic channel in response to flowing cells, we excited both coplanar- and planar-electrode sensor with 500 kHz sine wave and measured the resulting electrical current flow. In our measurement setup, we excited both sensors with the same AC signal from the common electrode (i.e., the surface electrode for the coplanar-electrode sensor and the blanket electrode for the parallel-electrode sensor), and acquired the current from the surface electrode for each sensor. The current signals from both sensors were first converted into voltage signals using transimpedance amplifiers, and then measured using a lock-in amplifier (Zurich Instruments HF2LI).

We compared the two sensor output waveforms containing signals for ~200 cells and found that the current modulation amplitude was 2~4× higher for the parallel-electrode sensor compared to the coplanar-electrode sensor for the same cell (Figure 6). These results agree well with our simulation results.

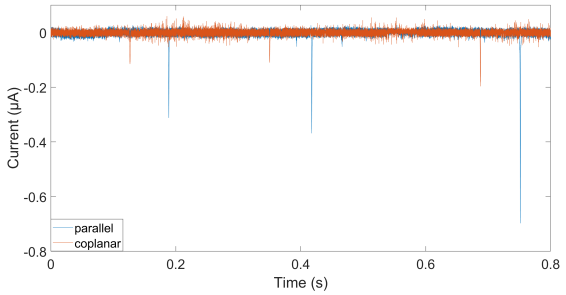

Figure 6: Electrical current modulation in response to the same cell recorded from a coplanar-electrode and a parallel-electrode sensor sequentially placed on the same microfluidic path. The microfluidic channel is 15 µm-high and 30 µm-wide. The peak signal amplitudes generated due to the same cell are 2~4× higher for the parallel-electrode sensor.

CONCLUSION

In this paper, we comparatively analyzed the performance of parallel-electrode Coulter sensor against the conventional coplanar-electrode Coulter sensor for microfluidic devices fabricated using soft lithography. Based on both computer simulation results and experiments with cell suspensions, we found that parallel-electrode Coulter sensor yields a higher sensitivity than the coplanar-electrode Coulter sensor, and the sensitivity enhancement is a function of the cell size, elevation, and microfluidic channel geometry.

ACKNOWLEDGEMENTS

This work is supported by National Science Foundation Award No. ECCS 1610995, ECCS 1752170, and the Beckman Young Investigator Award to A.F.S.

REFERENCES

[1] H. Zhang, C. H. Chon, X. Pan, D. Li, "Methods for counting particles in microfluidic applications", *Microfluid Nanofluid*, vol. 7, pp. 739-749, 2009.

[2] Y. Song, J. Zhang, D. Li, "Microfluidic and nanofluidic resistive pulse sensing: a review", *Micromachines*, vol. 8, 204, 2017.

[3] W. H. Coulter, "High speed automatic blood cell counter and cell size analyzer", *Proceedings Natl. Electron. Conference*, vol. 12, pp. 1034-1040, 1956.

[4] R. W. DeBlois, C. P. Bean, "Counting and sizing of submicron particles by the resistive pulse technique", *Rev. Sci. Instrum.*, vol. 41, pp. 909-916, 1970.

[5] R. Liu, N. Wang, F. Kamili, A. F. Sarioglu, "Microfluidic CODES: a scalable multiplexed electronic sensor for orthogonal detection of particles in microfluidic channels", *Lab Chip*, vol. 16, pp. 1350-1357, 2016.

[6] R. Liu, W. Waheed, N. Wang, O. Civelekoglu, M. Boya, C. H. Chu, A. F. Sarioglu, "Design and modeling of electrode networks for code-division multiplexed resistive pulse sensing in microfluidic devices", *Lab Chip*, vol. 17, pp. 2650-2666, 2017.

[7] N. Wang, R. Liu, A. F. Sarioglu, "Microfluidic platform with multiplexed electronic detection for spatial tracking of particles", *J Vis. Exp.*, vol. 121, e55311, 2017.

[8] R. Liu, N. Wang, N. Asmare, A. F. Sarioglu, "Scaling code-multiplexed electrode networks for distributed Coulter detection in microfluidics," *Biosens. Bioelectron.*, vol. 120, pp. 30-39, 2018.

[9] R. Liu, N. Wang, C. H. Chu, A. F. Sarioglu, "The effect of the electrode resistance on the performance of code-multiplexed resistive pulse sensing", 2017 *19th International Conference on Solid-State Sensors, Actuators and Microsystem (TRANSDUCERS),* Kaoshiung, June 18-22,2017, pp. 2115-2118.

[10] D. K. Wood, M. V. Requa, A. N. Cleland, "Microfabricated high-throughput electronic particle detector", *Rev. Sci. Instrum.*, vol. 78, 104301, 2017.

[11] R. Liu, C. Chu, M. Boya, O. Civelekoglu, H. Chen, A. F. Sarioglu, "Soft lithography compatible fabrication of parallel electrodes in microfluidic devices," in *Proc. of uTAS (The 22nd International Conference on Miniaturized Systems for Chemistry and Life Sciences)*, Kaoshiung, Nov. 11-15, 2018, pp. 825-827.

CONTACT

*A. F. Sarioglu, tel: +1-404-894-5032; sarioglu@gatech.edu